Mathematical Physiology: Notes on the Cable Equation

Frost

1 The Cable Equation

1.0.1 Background

To fully understand how neurons work, it's necessary to understand how a single nerve cell behaves. A neuron is composed of three parts: the dendrites, the cell body (soma), and the axon. Dendrites act as the receiver of information for the neuron and interact with other neurons. The soma contains the nucleus and mitochondria, and the output of the neuron goes through the axon. At the end of the axon there are synapses, which are cell junctions specialized in transmitting of electrical signals. An individual neuron through its dendrites might receive many signals from other neurons, call convergence, similarly can transmit a signal along its axons to many other neurons, called divergence. Spread of electrical current in a dendrite network is a passive process, that can be approximated as diffusion of electricity along a leak cable. The axon has a very excitable membrane that will propagate an electrical signal actively. While at the synapse, the membrane is specialized specifically for the release or reception of neurotransmitters.

1.0.2 Mathematics

For the network in which we are concerned it's unlikely that the membrane potential is the same at each point. In some cases spatial uniformity does occur but not generally. We will view the cell as a long cylindrical piece of membrane surrounding an interior of cytoplasm, the cable. We suppose everywhere the potential depends on length and not radial or angular distance so that the problem is one-dimensional. This is called the core conductor assumption. We will now divide the cable into a number of short pieces of isopotential membranes each of length dx long. All currents must balance in each section and there are only 2 kinds of current transmembrane and axial currents. The axial have intra- and extra-cellular components both which are assumed to Ohmic:

$$V_i(x+dx) - V_i(x) = -I_i(x) r_i dx$$

$$V_e(x+dx) - V_e(x) = -I_e(x) r_e dx,$$

where I_i, I_e are the intra- and extra-cellular currents respectively with the minus sign accounting for positive current follows the flow of positively charged ions. If $V_i(x+dx) > V_i(x)$ then the positive charge flows in the direction of decreasing x. That is, in the limit of $dx \to 0^+$ we have:

$$I_i = -\frac{1}{r_i}\frac{\partial V_i}{\partial x} \tag{1}$$

$$I_e = -\frac{1}{r_e}\frac{\partial V_e}{\partial x} \tag{2}$$

with r_i, r_e being the resistances per unit length of the intra- and extra-cellular media. In general, we will have $r_i = \dfrac{R_c}{A_i}$, where R_c is the cytoplasmic resitivity measured in units of Ohms - length and A_i is the cross-sectional area of the cylindrical cable. Following from Kirchhoff's Laws we get that any change in extra- or intra-cellular axial current must be due to a transmembrane current:

$$I_i(x) - I_i(x+dx) = I_t dx$$
$$I_t dx = I_e(x+dx) - I_e(x)$$

where I_t is the total transmembrane current (positive outward) per unit length of the membrane. Take the limit of $dx \to 0^+$ will give us the following:

$$I_t = -\frac{\partial I_i}{\partial x} = \frac{\partial I_e}{\partial x}$$

with no additional current sources the total axial current is $I_T = I_i + I_e$ so that $V = V_i - V_e$ giving us:

$$-I_T = \frac{r_i + r_e}{r_i r_e}\frac{\partial V_i}{\partial x} - \frac{1}{r_e}\frac{\partial V}{\partial x}$$
$$\frac{1}{r_i}\frac{\partial V_i}{\partial x} = \frac{1}{r_i + r_e}\frac{\partial V}{\partial x} - \frac{r_e}{r_i + r_e} I_T$$

finally this gives us the Cable equation (by noting a derivative in x gives us:)

$$I_t = \frac{\partial}{\partial x}\left(\frac{1}{r_i + r_e}\frac{\partial V}{\partial x}\right). \tag{3}$$

We used 1 and the fact that I_T is constant. Note that the transmembrane current I_t is a sum of the capacitive and ionic currents, and thus we obtain:

$$I_t = p\left(C_m \frac{\partial V}{\partial t} + I_{\text{ion}}\right) = \frac{\partial}{\partial x}\left(\frac{1}{r_i + r_e}\frac{\partial V}{\partial x}\right), \tag{4}$$

where p is the perimeter of the axon and $[C_m] = \dfrac{\text{Capacitance}}{\text{Area}}$ and $[I_{\text{ion}}] = \dfrac{\text{Current}}{\text{Area}}$ Now it's going to benefit us greatly if we non-dimensionalize this equation. Note the units $[R_m] = \Omega \cdot \text{cm}^2$. So that for fixed V_0, R_m is determined empirically by measuring the change in membrane current when V is perturbed slightly from V_0 mathematically that is:

$$\frac{1}{R_m} = \left.\frac{\partial I_{\text{ion}}}{\partial V}\right|_{V=V_0}.$$

Although R_m depends on chosen V_0, it's typical to just take V_0 to be resting membrane potential to define R_m. Note that if the membrane is an Ohmic resistor then we'll have $I_{\text{ion}} = \dfrac{V}{R_m}$, then R_m is independent of V_0. Assuming further that r_i and r_e are constant gives us a diffusive PDE:

$$I_t = \frac{1}{r_i + r_e}\frac{\partial^2 V}{\partial x^2} = pC_m\frac{\partial V}{\partial t} + I_{\text{ion}}$$
$$\iff \frac{R_m}{p(r_i + r_e)}\frac{\partial^2 V}{\partial x^2} = R_m C_m\frac{\partial V}{\partial t} + R_m I_{\text{ion}}.$$

Define a new parameter:

$$\lambda_m^2 = \frac{R_m}{p(r_i + r_e)} \qquad \tau_m = R_m C_m,$$

note that $[\lambda_m]$ = Length and that $[\tau_m]$ = Time. So that we will call these our length and time scales, respectively. Furthermore, assume that $r_e << 1$ so that:

$$\lambda_m = \sqrt{\frac{R_m}{p(r_i + r_e)}} = \sqrt{\frac{R_m d}{4R_e}},$$

where d is the diameter of the axon. Re-scale the ionic current by defining $I_{\text{ion}} = \dfrac{-f(V,t)}{R_m}$ for some function of voltage and time, f. Now we define the non-dimensional lengths and times:

$$X = \frac{x}{\lambda_m} \qquad T = \frac{t}{\tau_m},$$

respectively. This gives us the non-dimensional PDE:

$$\frac{\partial V}{\partial t} = \frac{\partial^2 V}{\partial x^2} + f(V,t),$$

generally, f is further reduced by assuming it's only a function of voltage.

2 Hodgkin and Huxley

2.0.1 Introduction

In Chapter 2 we described cell membranes as a capacitor in parallel with an ionic current resulting in:

$$C_m\frac{dV}{dt} + I_{\text{ion}}(V,t) = 0 \tag{5}$$

where $V = V_i - V_e$. In an axon, similar to many neural cells, the principal ionic currents are the Na^+ (Sodium) and K^+ (Potassium) currents. There are others, but Hodgkin-Huxley lumps them together into a "leakage current". Since the instantaneous I / V curve of open Na^+ and K^+ channels are approximately linear (5) gives:

$$C_m \frac{dV}{dt} = -g_{Na}(V - V_{Na}) - g_K(V - V_K) - g_L(V - V_L) + I_{app}, \tag{6}$$

where I_{app} is the applied current. During an action potential there's a measured influx of Na^+ (Sodium) and a subsequent efflux of K^+. There amounts are small, so its reasonable to assume ionic concentrations imply equilibrium potentials are constant and unaffected by an action potential. The graph I/V being linear is chosen by experimental data however this behaviour can differ based on species. Equation (6) is a first-order ODE:

$$C_m \frac{dV}{dt} = -g_{eff}(V - V_{eq}) + I_{app}, \tag{7}$$

where $g_{eff} = g_{Na} + g_K + g_L$ and $V_{eq} = \dfrac{g_{Na}V_{Na} + g_K V_K + g_L V_L}{g_{eff}}$. That is, V_{eq} is the resting potential and is a balance between the reversible potentials for the 3 ionic currents. At rest, the Na^+ and leakage conductance are small compared to K^+ conductance, so that the resting potential is close to the K^+ equilibrium potential. Define $g_{eff} = \dfrac{1}{R_m}$ as the passive membrane resistance and it's $R_m = O(1000)[\Omega \cdot cm^2]$ with $\tau_m = O(1)[ms]$ so that we have an equilibrium with a steady applied current giving:

$$V = V_{eq} + R_m I_{app}$$

Assuming 6 is correct the only possible explanation for the differences is that conductance's aren't constant but depend on voltage. The key step was then to measure induced ionic currents and deduce changes in conductance.

2.0.2 History

Hodgkin and Huxley determined the dynamic ionic conductance that generate nerve action potential. Previous to 1939 it was believed that membrane potential played an important role in the membrane's state but there was no measurements. It was known that a cell's membrane separated into different ionic concentrations inside and outside of the cell. Applying the Nernst equation, Bernstein suggested that the resting membrane was semipermeable to K^+ so that at rest V should be around $-70[mV]$. He believed that during activity there was a breakdown in the membrane's resistance to all ionic fluxes, and the potentials would vanish. It was measured by Cole and Curtis that a substantial transient increase in membrane

conductivity during action potential took place, but it wasn't infinite. Eventually Curtis and Hodgkins succeeded in measuring V directly. They found V rose transiently toward zero, but with a big overshoot. They developed the space-clamp technique, this allowed direct measurement of the total transmembrane current. This was done by attaching a silver wire to the axon to act as a metal conductor to provide for axial resistance and thereby eliminate voltage gradients along the length of the axon. This makes the membrane potential no longer dependent on space, just time. And progress was made on controlling membrane potential. Eventually the measured transient ionic fluxes over the physiological relevant ranges. They then identified the individual contributions of Na^+ and K^+ and explained the over shoot before zero during action potential. This suggested there was a transient increase in permeability identical for all ions, they realized that different changes in permeability for different ions could account for the V time course, as V would approach Nernst potential for the ion to which the membrane was predominantly permeable and this dominance would change with time. An example, at rest the membrane is most permeable to K^+ so V is close to V_K. However, if g_K decreases and g_{Na} were to increase, then V would be pushed towards V_{Na} which is positive and depolarization of the cell occurs. The remaining question of how changes in permeability were dynamically linked to V was not completely stated in their paper.

2.0.3 Voltage and Time Dependence of Conductance

The main development in figuring out the dynamics of the conductance came from the Voltage clamp, which fixes the membrane potential usually by a rapid step from one level of voltage to another. Since the supplied voltage must equal the transmembrane current, the voltage clamp provides a way to measure the transmembrane current that results. That is making voltage a step-wise function its easy to measure ionic currents, thus even when conductance are functions of voltage, a voltage clamp prevents changes in voltage and permits measurement of the conductance as functions of time only. When voltage was stepped up and held fixed at a higher level, the total ionic current was initially inward: They argued that initial inward current was carried by Na^+ and outward by K^+. They replaced 90% of all extracellular Na^+ in the saltwater both with Choline which rendered the axon non excitable but changed the resting potential only slightly. It was assumed that immediately after the voltage was stepped up that ionic current carried by Na^+ could be measured in response to the voltage increase. They can be measured immediately but usually not in long time, since K^+ current begins to contribute. Denote the 2 cases Na^+ with Normal and zero extracellular by I^1_{Na} and I^2_{Na}, respectively, then:

$$\frac{I^1_{Na}}{I^2_{Na}} = K.$$

Two further assumptions were made:

The Hodgkin-Huxley Model

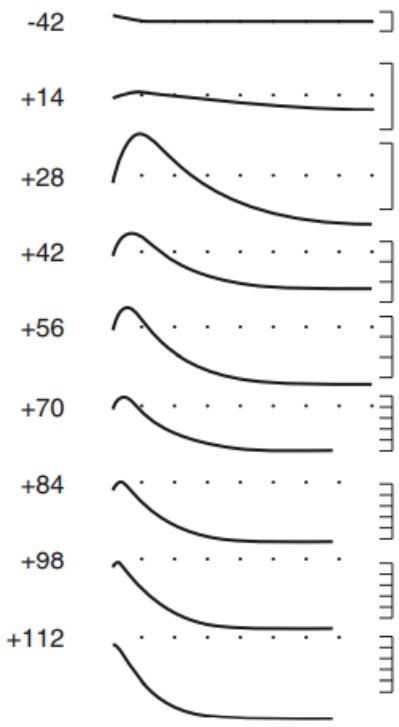

Figure 5.2 Experimental results describing the total membrane current in response to a step depolarization. The numbers on the left give the final value of the membrane potential, in mV. The interval between dots on the horizontal scale is 1 ms, while one division on the vertical scale represents 0.5 mA/cm^2. (Hodgkin and Huxley, 1952a, Fig. 2a.)

Figure 1: Note the Inward curve

1. Na^+ current ratio K is independent of time and is thus constant over the course of each Voltage clamp experiment. That is, amplitude and direction of the Na^+ current may be affected by low extracellular solution but its time course is not.

2. Second, they assumed that K^+ channels are affected by the change in extracellular Na^+ concentration. There's a lot of evidence for Na^+ and K^+ to be independent.

TTX is known to block Na^+ currents while K^+ current remains almost unaffected but TEA has the opposite effect of blocking the K^+ current but not the Na^+ current. Since

$$I_{ion} = I_{Na} + I_K \tag{8}$$
$$I_K^1 = I_K^2, \tag{9}$$

so that it follows that:

$$I_{ion}^1 - I_{Na}^1 = I_{ion}^2 - I_{Na}^2 \tag{10}$$
$$\implies I_{Na}^1 = \frac{K}{K-1}(I_{ion}^1 - I_{ion}^2) \tag{11}$$
$$\implies I_K = \frac{I_{ion}^1 - K I_{ion}^2}{1-K}. \tag{12}$$

So that given I_{ion} and K (the ratio of sodium currents) it's possible to determine the courses for both Na^+ and K^+. We can also get the conductance:

$$g_{Na} = \frac{I_{Na}}{V - V_{Na}} \qquad g_K = \frac{I_K}{V - V_K} \tag{13}$$

This relies on the linear model used to describe the I/V curve of the Na^+ and K^+ channels. The important note is that the voltages held fixed, conductance is time-dependent. Example, V is stepped up and held fixed at a higher level J_K doesn't instantaneously increase, but instead increases to a steady state in long time. It increases at first and then decreases after a hump, this is described as sigmodial. g_{Na} is more complicated.

2.0.4 Potassium Conductance

From experimental data it's reasonable to conclude:

$$\frac{dg_K}{dt} = f(v,t),$$

where $v = V - V_{eq}$ (V_{eq} is the resting potential) so that $\dfrac{dv}{dt} = \dfrac{dV}{dt}$. But it was easier to write g_K as some power relationship since it was sigmodial:

$$g_k = \bar{g_k} n^4,$$

$\bar{g_K}$ is constant. The power 4 is the smallest power where the curve fits the data. n then must satisfy

$$\tau_n(v)\frac{dn}{dt} = n_\infty(v) - n, \tag{14}$$

$n_\infty(v)$ and $\tau_n(v)$ must be empirically determined and is equivalently

$$\frac{dn}{dt} = \alpha_n(v)(1-n) - \beta_n(v)n, \tag{15}$$

with $n_\infty(v) = \dfrac{\alpha_n(v)}{\alpha_n(v)+\beta_n(v)}$ and $\tau_n(v) = \dfrac{1}{\alpha_n(v)+\beta_n(v)}$. At elevated potentials $n(t)$ increases monotonically and exponentially towards its resting value, thereby turning on, or activating K^+ current. The Nernst potential is below the resting potentials, the K^+ current potentials greater than rest. The function $n(t)$ is called the K^+ activation.

But how does this give the sigmodial nature of g_K? Suppose at $t = 0$, v increased from 0 to v_0 and holds constant and suppose n is at steady state when $t = 0$: that is $n(0) = n_\infty(0)$. Assume $n_\infty(0) = 0$:

$$n(t) = n_\infty(v_0)\left[1 - \exp\left(\frac{-t}{\tau_n(v_0)}\right)\right]$$

which is an increasing curve that approaches $n_\infty(v_0)$ as $t \to \infty$. Raising n to the 4^{th} power gives the desired behavior.

In the case of a step decrease from then the solution is:

$$n(t) = n_\infty(v_0)\exp\left(\frac{-t}{\tau_n(0)}\right)$$

from $v_0 \to 0$ in which case n^4 is exponentially decreasing. To derive n_∞ and τ_n from the data, this is done for a fixed value of $V - V_{eq} = v$ and whatever continuous functions that fit the data would be suitable.

2.0.5 Sodium Conductance

The time dependence of g_{Na} is a more difficult problem. One process turns the current Na^+ on and the other off. They suggested:

$$g_{Na}(v) = \overline{g_{Na}}m^3h,$$

where

$$\frac{dw}{dt} = \alpha_w(1-w) - \beta_w w,$$

where $w = m$ or h. m is small at rest and first increases, it's called the sodium activation variable and h shuts it down so its called sodium inactivation variable. When $h = 0$, Na^+ is completely shut down. Similar to g_K for fixed voltage step, α_w, β_w are determined by fitting to an experimental data set.

2.1 Summary of the Equations

The Hodgkin Huxley equations for space-clamped axon are:

$$C_m\frac{dv}{dt} = -\overline{g_K}n^4(v-v_k) - \overline{g_{Na}}m^3h(v-v_{Na}) - \overline{g_L}(v-v_L) + I_{app} \tag{16}$$

$$\frac{dm}{dt} = \alpha_m(1-m) - \beta_m m \tag{17}$$

$$\frac{dn}{dt} = \alpha_n(1-n) - \beta_n n \tag{18}$$

$$\frac{dh}{dt} = \alpha_h(1-h) - \beta_h h \tag{19}$$

with experimental data suggesting:

$$\alpha_m = 0.1\frac{25-v}{\exp\left(\frac{25-v}{10}\right)-1} \tag{20}$$

$$\alpha_h = 0.07\exp\left(-\frac{v}{20}\right) \tag{21}$$

$$\alpha_n = 0.01\frac{10-v}{\exp\left(\frac{10-v}{10}\right)-1} \tag{22}$$

$$\beta_m = 4\exp\left(\frac{-v}{18}\right) \tag{23}$$

$$\beta_h = \frac{1}{1+\exp\left(\frac{30-v}{10}\right)} \tag{24}$$

$$\beta_n = 0.125\exp\left(\frac{-v}{80}\right), \tag{25}$$

The Hodgkin-Huxley Model

with $v = V - V_{eq}[mV]$, with the following units, current density $\left[\frac{\mu A}{cm^2}\right]$, conductance $\left[\frac{mS}{cm^2}\right]$, and capacitance $\left[\frac{\mu F}{cm^2}\right]$. Additionally the following parameters were found to fit the data:

$$\begin{aligned} \overline{g_{Na}} &= 120 & v_{Na} &= 115 \\ \overline{g_K} &= 36 & v_K &= -12 \\ \overline{g_L} &- 0.3 & v_L &= 106 \\ & C_m = 1. \end{aligned}$$

We showed with Hodgkin and Huxley derived by modeling the ionic channels as consisting of multiple sub units each obey a simple two-state model. The Hodgkin-Huxley equations for Na^+ gating equations can be derived from the assumption that the Na^+ channel consists of three m-gates and one $h-$gate, each are either open or closed. If they operate independently, then the fraction of open Na^+ channels is m^3h where m, h obey the equation of the two-state channel models. If there are 4 $n-$gates per K^+ channel all of which must be open for K^+ to flow, then the fraction of K^+ channels is n^4.

Is this previous work we've done realistic? If we apply small currents to a cell for a short time, the potential returns rapidly to its equilibrium $v = 0$ after the current is removed. There's always a competition among the 3 ionic currents to drive potential to their corresponding resting potential. If K^+ and the leakage current are blocked or the Na^+ conductance increases dramatically, then the term $\overline{g_{Na}}(v - v_{Na})$ should dominate (16) and so long as $v < v_{Na}$ an inward Na^+ current would drive the potential $v \to v_{Na}$. Notice since $v_K < v_L < v_{Na}$, v is in range $v_K < v < v_{Na}$.

If g_{Na} and g_K are constants, the equilibrium would be at $v = 0$ and be stable and the potential would return exponentially to rest. But since they aren't constant, the different currents can exert their influences differently. The action outcome is determined by the equations on m, n, h. The important thing to note is $\tau_m(v) << \tau_n(v)$ and $\tau_m(v) << \tau_h(v)$, so then $m(t)$ responds quickly to changes in v compared to n and h. If the potential v is slightly raised by a small stimulating current then the system returns to stable equilibrium. During that period of time that v is elevated, Na^+ activation m tracks $m_\infty(v)$. If the stimulating current is large enough to raise the potential and therefore $m_\infty(v)$ is at a high enough level, then before the system returns to rest, m will increase sufficiently to change the sign of the net current, resulting in an auto catalytic inward Na^+ current. As the potential rises, m continues to rise and the inward Na^+ current is increased, further adding to the rise of the potential.

If nothing else would happen v would be driven to v_{Na}. However, time constants become important here. When the potential is at rest, Na^+ inactivation variable h is positive and as the potential increases $h_\infty \to 0$ and as $h \to 0$ Na^+ is inactivated because $g_{Na} \to 0$. However because $\tau_n(v) >> \tau_m(v)$ there's a large delay between turning on Na^+ and turning off Na^+

current, the net effect is two different time scales of m and h is that the Na^+ current is first turned on and later off and this is seen as the initial increases of the potential, followed by a decrease towards rest.

At the same time Na^+ is inactivated the outward K^+ current is activated, because $\tau_n(v)$ and $\tau_h(v)$ and their similarity. Activation of K^+ drives the potential below rest towards v_k. When v is negative, n declines, and the potential eventually returns to rest and the process starts again.

There are 4 stages to action potential: upstroke, excited, refractory, recovery. Refractory following excited phase when no additional stimuli evokes no substantial response, even though the potential is below or close to its recovery phase. There can't be a response, since the Na^+ channels are inactivated because h is small. As h gradually returns to rest, further responses become possible.

2.1.1 Oscillations in the Hodgkin-Huxley Equations

There are 2 ways Hodgkin-Huxley has a steady limit cycle. First inject a steady current of sufficient strength, by increasing I_{app}. Such a current will raise the resting potential above the threshold for an action potential, so that after the axon has recovered from an action potential, the potential rises to a super-threshold level at which another action potential is evoked. Note that in 2 as I_{app} increases so does v and the steady state is table for $I_{app} < 9.78$ at which point it becomes unstable and decays into a sub-critical Hopf bifurcation. The bifurcation gives rise to a branch of unstable limit cycle oscillations which bends backward initially. Unstable limit cycles are drawn with dashed lines and stable with solid. In $(5.7(A))$ we also plot the minimums and maximums of oscillations as functions of I_{app}. The branch of unstable limit cycles terminates at a limit point where it coalesces with stability. The stable periodic solutions are observed by direct calculation. At layer values of I_{app} the limit cycles disappear into another Hopf bifurcation, this time at a super-critical one leaving only stable steady states.

Immersing the axon in a bath of high extracellular K^+ has the same effect through a different mechanism. Increased extracellular K^+ has the effect of increasing K^+ Nernst potential, raising the resting potential. If the increases of K^+ Nernst potential is large, the resting potential becomes super threshold and autonomous oscillations result. This mechanism of creating an autonomous oscillator out of normally excitable but non-oscillatory cells is important for cardiac arrhythmia.

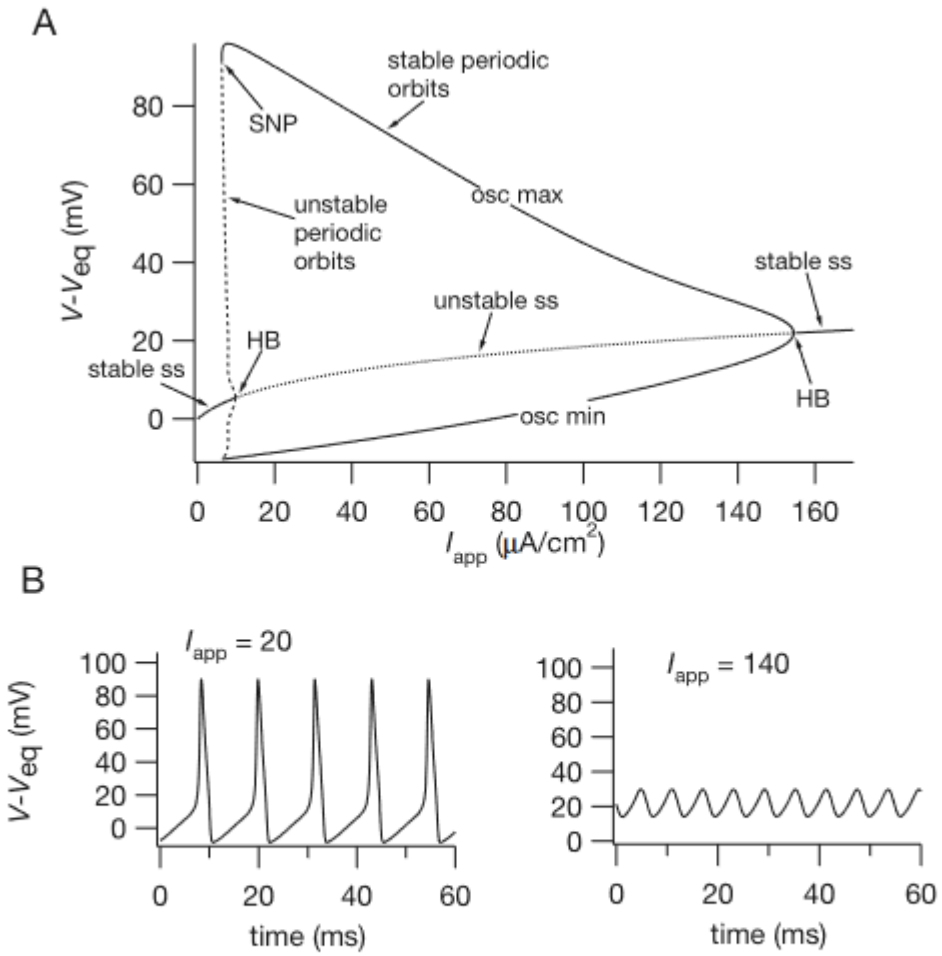

Figure 5.7 A: Bifurcation diagram of the Hodgkin–Huxley equations, with the applied current, I_{app} as the bifurcation parameter. HB denotes a Hopf bifurcation, SNP denotes a saddle-node of periodics bifurcation, osc max and osc min denote, respectively, the maximum and minimum of an oscillation, and ss denotes a steady state. Solid lines denote stable branches, dashed or dotted lines denote unstable branches. B: Sample oscillations at two different values of I_{app}.

Figure 2: Courtesy of Mathematical Physiology (Keener & Synder)

3 A Simple 2D Model of Cardiac Tissue Conduction

3.1 Introduction

The cardiac conduction system is made up of pacemaker cells, specialized conduction cells and myocytes. Under normal conditions the sinus node in the right atrium generates the signal to contract. The signal is conducted to the right and left atrium and enters the atrioventricular node (AV node). The AV node initiates conduction of the signal to both the right and left "bundle branches". The contraction of both start from the bottom and maximizes the ejection of blood through the arteries and aorta.

At the cellular level, voltage gated channels and gap junction are responsible for generation and propagation of action potentials in cardiac tissue, respectively. This starts with phase 0upstroke depolarization resulting from the activation of voltage-gated Na^+ channels and resulting influx of Na^+ ions due to a depolarizing current spread through adjacent cells through gap junctions. The next phase results from opening of K voltage gated channels allowing an ion K^+ efflux. The action potential plateau, phase 2, is due to the Ca^{++} ions through the voltage gated Ca^{++} channels as well as the efflux of K^+ ions through K^+ voltage gated channels. The depolarization of myocyte, phase 3, is cause by K^+ ions efflux through K^+ voltage gated channels once Ca channels are inactivated. Phase 4 is the resting stage of myocyte, which is driven by K^+ transmembrane gradient generated by Na^+ and K^+ pump at negative resting potential.

Cellular automata (CA) provides a natural way of modeling local behavior and interactions. The space is discretized into patches or cells that are capable of having a finite number of states. Each cell is given a probability of interacting with cells around it. Every cell has its own state and rules are shared amongst all of them. Each time step the rules are imposed and a time series emerges. The advantage of this as opposed to other techniques is that it's simple to implement a rule based system. This is compared to the large system of ODE's or PDE's that might be required elsewhere. These also rely on homogeneous actors and spatial aspects are difficult to capture.

In-vivo experiments being impossible to preform CA provides a good alternate. This also allows for understanding of arrhythmia's. This information obtained by studying the individual channels and various electrocyte concentrations can be utilized to develop step-wise rules used to create the CA An accurate CA model will allow for easy experiments and analysis.

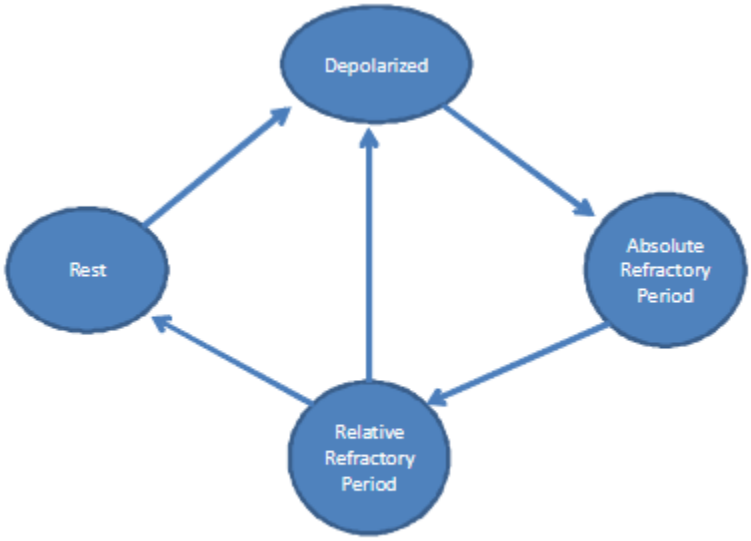

Figure 2: State diagram of the virtual myocytes

Figure 3: Menke et. al. 2007

3.2 Materials and Methods

The CA model here is a 2D excitable media model. One in which for each cell there's a unique rest state which may be perturbed into an transient excited state that relaxes back to rest. The cell is unable to be re-excited during a refractory period. In this case, the grid of cells is in the shape of a torus allowing cells across the boundary to interact. Therefore boundary conditions are not necessary. The patches are ventricular myocytes. The grid is 16×16. The neighborhood is a Neumann one with 4 neighbors per cell. The grid is designed to stimulate a single ventricle in which, given the lack of B.C's waves of electrical activity are sustainable. The specialized conduction cells aren't included as they aren't needed for signal propagation given the size of the system. The AV node pacemaker is simulated by a depolarizing signal sent by a row of cells that occurs at a defined rate. Each tick is $1[ms]$. The following assumptions are made:

- Ventricle myocytes (patches) are capable of 40 beats per minute
- Na^+ channels open time is user defined in the range $1 - 10[ms]$.
- Ca^{++} opening time is user defined in the range $200 - 400[ms]$
- QT_c is a user defined variable in the range $300 - 1000[ms]$, this controls the K^+ channel

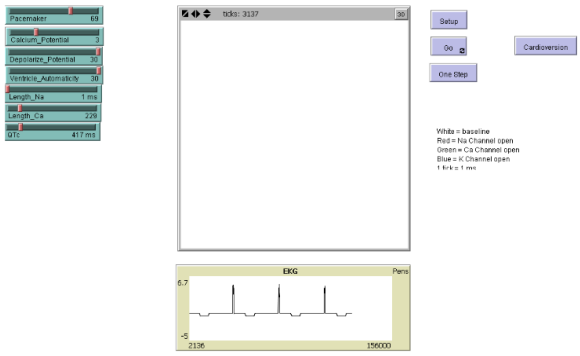

Figure 3: NetLogo User interface for cardiac conduction model

Figure 4: Menke et. al. 2007

opening time and repolarization time.

- The myocyte goes from a state of rest at $-90[mV]$ to depolarization $30[mV]$ upon exposure to depolarizing current $-55[mV]$. The enters an absolute refractory period once the electrical potential reaches $-65[mV]$. The cell then enters the rest state at a rate that's determined by QT_c. The user also inputs depolarizing potential and the calcium channel potential.

The user input is shown in (**??**)

3.3 Results

Given normal parameters of heart, length of Na^+/Ca^{++} channel opening times and QT_c, the CA models a normal heart rate. This occurs without any pathological dysrhythmias over many heart beats. The EKG graph is normal and the state space of x_t/x_{t+1} is a stable orbit when QT_c levels are normal.

Upon increasing QT_c, the model enters an unstable tachycardia. Where the rate of ventricle depolarization from $120[bpm] - 180[bpm]$. The resulting EKG is irregular in (5) and the state plot enters into a tachyarrhythmia which cannot be escaped (6)

3.4 Discussion

Cellular Automata provides a non-reductionist way of studying biological systems as a whole, while retaining individual levels of information. The results back up that the cardiac conduction system can be simulated using cellular automata. The advantage of using CA is that

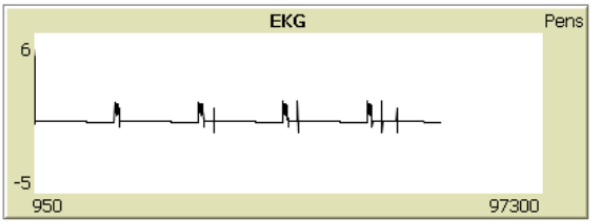

Figure 7: Abnormal EKG with AV dissociation

Figure 5: Menke et. al. 2007

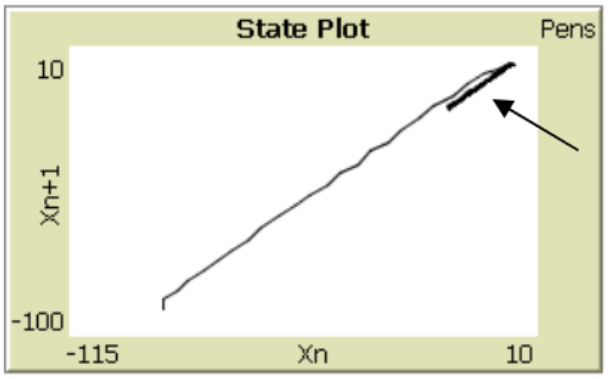

Figure 6: State plot of the electric potential. The arrow demonstrates the creation of a ventricular tachycardia and the inability to escape after its generation

Figure 6: Menke et.al. 2007

we can monitor conditions like the electrical potential of each myocyte as depolarization and repolarization occurs. This implies that a large number of factors that influence conduction e.g. electrolyte concentrations, congenital and acquired alterations in voltage gated channels, and ischemia inducted changes in conduction, can be readily simulated. This CA approach provides the ability to simulate the effect of anti-arrhythmic medications and ischemia at the cardiac myocyte and tissue level.

4 A Computational Model of Invasive Aspergillosis In the Lung And The Role of Iron

4.1 Background

Invasive aspergillosis affects $372k$ in 2007 and despite drugs has a fatality rate of 30%. Recent records of drug resistances has the possibility of a perfect storm. Iron homeostasis plays a critical role in the biology of Aspergillosis. Aspergillosis species adapts to iron-limited environments by activating scavengers (intracellular) to find iron and store it. From studies the siderophores remote iron from transferring in Human serum and impair macrophage iron uptake, conversely neutrophil lactoferrin inhibits aspergillosis. In summary competition for iron is a key component of the pathogenesis of invasive aspergillosis.

Innate immune response to invasive aspergillosis is difficult to study. Interrogating dynamic cellular/molecular networks in humans is most often impossible. Some in vitro/in vivo methods have been successful with Aspergillosis however. Animal models have been easier to study as well. Neutrophils, macrophages, dendritic cells and lung epithelial cells are key players in host response to Aspergillosis species. Focus has been on fungal targets, for therapeutics, but recent developments promise host immunity might be a better strategy. This requires a better understanding to the current response of the body. Dynamic regulatory molecular networks and multi-scale nature of the problems make this difficult. We focus here on the tissue-level component of the model, validated with in vivo data from a mouse model of invasive aspergillosis.

4.2 Related Work

ABMs are well suited for heterogeneous immune systems. Some references for agent-based modeling:

- Chavali AK, Gianchangani EP, et.al. 2008
- Baver et. al 2009 (focused on review of host-pathogen ABMs)

It's been established that pathogen distribution and spatial scale are important factors. Chemotaxis has been found to be the most effective strategy for neturophils finds A. fumigatus conida. This model incorporates specific spatial structures as well as respiratory effects and provides data on macrophage recruitment time and mechanism for chemokine diffusion. Our model incorporates both macrophages and neutrophilis, using chemokine diffusion and chemotaxis in a spatially heterogeneous domain to investigate the immune response to aspergillosis over time. As well as introduction iron as a key factor in the survival of the fungus.

5 Methods

Skipped over, goes through experimental design.

5.1 Results and Discussion

5.1.1 The Simulation Model

Built in Net Logo the model consists of a 3D subsection $400[\mu m] \times 200[\mu m] \times 200[\mu m]$ of lung tissue consisting of an alveolar duct, for adjacent capillaries and surrounding lung parenchyma. A. fumigatus conidia enters at one end of the alveolar duct, as the simulations progresses the conidia drift through the airway. ABM simulates the epithelial clearance via a parameter dictating the probability of conidia lodging in the epithelium. Left undisturbed, conidial spores enter a swelling phase prior to germination, so that hyphal clusters begin to grow into the adjacent lung interstitium. In vivo, antimicrobial compound in the airway surface fluid act as the first line of defense against conidia, occasionally conidia that aren't cleared in this way can invaded the interior of epithelial cell; this simulation also allows epithelial cells to internalized, damage, and kill conidia.

Epithelial cells act as a second line of defense against A. funigatus. These recognized the presence of conidia and release inflammatory cytokines to the interstitial space in order to initiate an immune response. There are 2 immune types in the ABM: recruited monocytes/-macrophages and neturophils. We represent epithelial cells as releasing two-types of chemotactic factors, for neutrophils and monocytes/macrophages, respectively. These chemotactic factors were tracked seperately based on the literature and represent the aggregation of cytokines to which the respective immune cell types respond. The levels of fungal burden as measured by the number of conidia and hyphae. The chemotactic factors diffuse through the interstitial tissue eventually reaching local capillaries. Recruitment of leukocytes adhere to the capillary vascular endothelium occurs when the local concentration for a particular immune cell rises above some threshold.

Recruited immune cells enter the interstitial space via the bloodstream. There chemotaxsis is simulated as the immune cells follow the gradient of the concentrations of the chemotactic factor, a movement mechanism detailed in the references [27,28,60]. At the source of the gradient, the immune cells are attached. Macrophages may internalize several fungal cells. Once this happens cells are prohibited from escaping and from germinating. Over time these fungal cells are damaged and finally destroyed. Damage by macrophages is limited by the number of internalized fungal cells, while neutrophil damage is limited by the number of available granules.

In the absence of sufficient chemotactic factors, immune cells will move rapidly throughout the tissue. Since the lifetime of neutrophlis is short 24 to 48 hours neutrophilis are represented as dying after this period. Macrophages leave the represented cross section with no conidial spores remaining.

A key factor of the model is fungal acquisition of iron: the immune response induces hemorrhage, causing tissue iron level to increase. The fungus is able to acquire the iron both from the store of free iron and via a siderophore system. Iron will be modeled by diffusing throughout the tissue. Once a threshold of iron is reached for a cell, the new hyphal cell will grow. When a neutrophils encounters a hyphal cell, it will immediately sequester all iron in the immediate area. If the immune system fails at stopping this iron acquisition the fungus will consequently grow and aspergillosis develops.

The simulation continues in this manner until stopped at a predetermined time. This modeling of the immune response and Aspergillosis is the ABM. The parameter will be discussed below.

5.1.2 Parameter Sensitivity

4 quantities have been chosen from the ABM to compare to real data: fungal burden, iron level throughout the tissue space, macrophage cell counts, and neutrophil cell counts. Normal immune system responses are also evoked and neutropenia is modeled by first in the 48 hour of neutrophils being present, then it resumes to normal levels during the remainder. Many processes in this model are pseudo random averages and standard deviations are used to measure many quantities involved. For 20 runs all data except fungal growth was reliable, 40 runs were ran to have all data reliable which was compared to 200 runs and the difference was small.

Many state variables were obtained from literature, 9 parameters were left to fit to the data. These parameters were picked at a baseline and then adjusted to tune to data. This was done under healthy and neutropenic conditions.

Overall model dynamics were not effected by 3 of the 9 parameters, cytokines production factor, a unit-less multiplier that determined the number of macrophages and neutrophil-

specific cytokines that are produced by epithelial cells in response to fungal presence. The lack of an effect is likely due to macrophages and neutrophils following cytokine gradients to determine movement; since chemotaxis is simulated based on relative levels of nearby cytokines, the multiplier isn't critical. The second, is a proportion of nearby cytokines that are taken up by receptors on macrophages and neturophils. Lack of significance is possibly due to cytokine uptake doesn't have a sufficiently large effect on the relative nearby cytokine concentration to alter cell movement. The final parameter that has little effect is the recruitment threshold which determines both minimal amount of cytokines that must be present for macrophages and neutrophils to move according to chemotaxis (if below threshold they move randomly) and the possibility for new macrophages and neutrophlis to appear in the blood (new immune cells appear only if their respective cytokine levels are below threshold). In all 3 cases the scaling parameter had little effect on dynamics.

4 other parameters had quantitative differences but no qualitative:

4. Probability of conidial spores lodging in the epithelium - think strength of the cilia in sweeping away fungus
5. Proportion of available iron that is absorbed by fungal cells
6. Iron needed in order for fungus to grow
7. Detection radius, which determines how close immune cells need to be for fungal detection

The last item above was the most sensitive to model dynamics. This was explained away by Net Logo's distance handling, as $12[\mu m]$ only considered the single cell in simulation while $15[\mu m]$ expanded that neighborhood to 26 cells.

The last 2 parameters were:

8. Diffusion rate of iron and cytokines throughout tissue. This saw less iron being consumed as fungal cells died off and no change in macrophage counts.
9. Maximum amount of iron that fungal cells can store. This determines the effective growth rate of the fungus as less means the fungus does not have enough iron to grow.

These parameters were considered for immunocompotent and neutropenic situations, see the original paper for values determined.